



Cryogenic Cofired Multilayer Actuator Development for a Deformable Mirror in the Next Generation Space Telescope

MAUREEN L. MULVIHILL,* RYAN J. SHAWGO, ROGER B. BAGWELL & MARK A. EALEY

Xinetics, Inc., 37 MacArthur Avenue, Devens, MA 01432, USA

Submitted October 10, 2001; Revised March 28, 2002; Accepted June 6, 2002

Abstract. Xinetics is working with NASA to develop a cryogenic deformable mirror technology to meet the specific needs of the Next Generation Space Telescope. One of the critical technical issues is the development of a cryogenic actuator with sufficient displacement and temperature stability. This paper discusses the two year effort to achieve a cofired electroceramic multilayered cryogenic actuator. The development began by testing materials from 300 to 35 K via a cut and bond actuator technology that led to a cryogenic electroceramic material down selection. After selecting a doped SrTiO₃, a cofired actuator process specific to the cryogenic ceramic was developed. The assembled cryogenic actuators achieved the 3 μm displacement (stroke) between 35 and 65 K required by the deformable mirror design. The discrete cryogenic actuators were assembled into an engineering model cryogenic 349-channel deformable mirror that was delivered to NASA in October 2001.

Keywords: multilayer actuators, cryogenic actuators, next generation space telescope, adaptive optics, deformable mirror

1. Introduction

Presently, NASA and its partners are designing the Next Generation Space Telescope (NGST) as the follow-on space astronomy observatory to the Hubble Space Telescope [1] which is expected to launch in 2009. The design requirements include a large primary mirror (6–8 meters in diameter), an orbit at the second Lagrange Point (L2) and an operation temperature between 35 and 65 K. The large primary mirror requires that the telescope must be deployable after launch. Since the L2 point is 1.5 million kilometer outside Earth's orbit, the telescope will be unserviceable by the space shuttle. NGST must be maintained at cryogenic temperatures because of the infrared detectors that will be used in the science instrument module.

Active optics on NGST are considered a necessity since NGST's orbit will be unserviceable by the space shuttle and from the lessons learned from the Hubble Space Telescope that was "fixed" with the installation of the Wide-Field/Planetary Camera II [2]. A cryogenic

deformable mirror (DM) could correct potential static aberrations due to misalignments of the primary mirror petals after deployment or optical surface errors after launch due to gravity changes [3]. From an astronomy perspective, it could be used to enhance the resolution of point objects.

Xinetics has been contracted by NASA to develop a cryogenic DM technology specific to the needs of NGST through a series of pathfinder hardware demonstrators. Of utmost importance was the development of an electrostrictive cryogenic actuator with operation capability between 35 and 65 K. Under NASA contract number NAS8-98073, three pathfinder cryogenic DMs were built using cut and bond actuator technology, shown in Fig. 1. NASA contract number NAS8-99129 funded a cryogenic 349-ch engineering model DM assembled using cofired cryogenic actuators, shown in Fig. 2. This paper describes the two-year cryogenic cofired multilayer actuator technology development from the cryogenic electrostrictive ceramic down selection and the cut and bond actuator testing to the cofired cryogenic actuators development and assembly. The goals of the discrete cryogenic

*To whom all correspondence should be addressed.

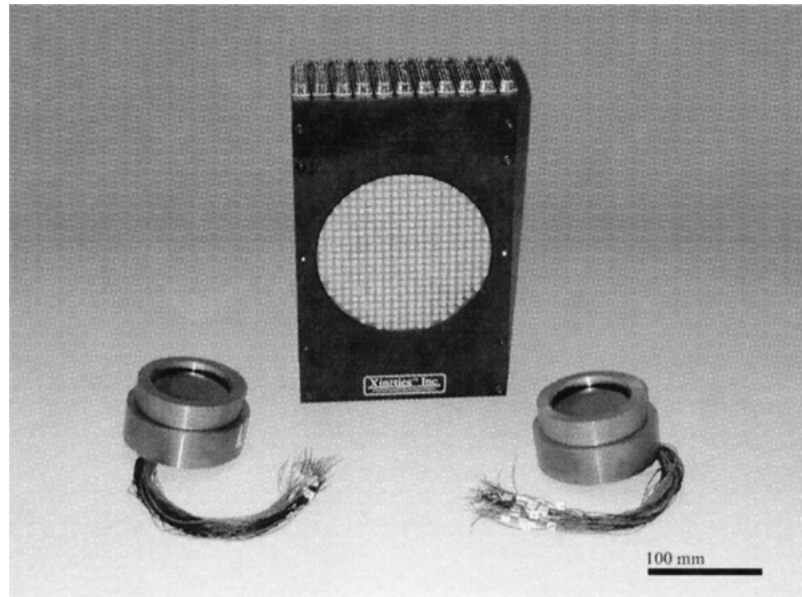


Fig. 1. Deformable mirror hardware demonstrators delivered under NASA contract number NAS8-98073. A 349-ch cut and bond discrete actuator cryogenic DM ($234 \times 76 \times 183\text{-mm}^3$) and two 37-ch cut and bond discrete actuator cryogenic DMs (both are 102 mm in diameter \times 38 mm in depth).

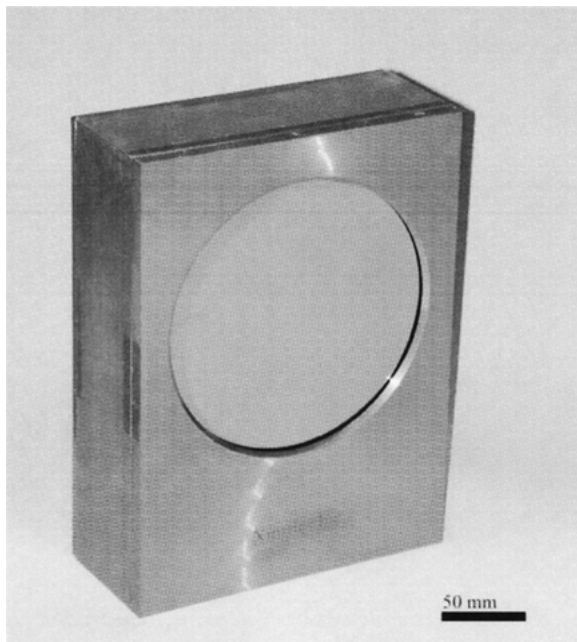


Fig. 2. 349-ch cryogenic discrete cofired actuator deformable mirror ($246 \times 61 \times 185\text{ mm}^3$) delivered under NASA contract number NAS8-99129.

actuators between 35 and 65 K were achieved: a $3.0\ \mu\text{m}$ displacement and a negligible hysteretic response suggesting an electrostrictive material.

2. Experimental Procedure

Two techniques are traditionally used to assemble multilayer actuators: the cut and bond technique (C&B) and the cofire technique [4]. The C&B technique requires a small amount of powder ($\sim 50\ \text{g}$) and a water soluble binder to assemble one test actuator. The fabrication of a cofired test actuator requires a large powder quantity ($\sim 1000\ \text{g}$) and the development of a compatible binder system specific to the powder properties. The C&B technique was selected as the method to assemble the test actuators for the composition studies. A considerable amount of unnecessary research and development time was avoided since the batch sizes were less than 100 g and a water based binder system was used when necessary. Once a promising composition was identified, a cofired process specific to that composition was developed.

2.1. Cryogenically Active Materials Evaluations

Landolt and Börnstein [5] was used to select materials that exhibited large dielectric constant below

100 K. The investigations centered on doped SrTiO_3 and KTaO_3 in single and polycrystalline forms. The single crystals were SrTiO_3 ,¹ KTaO_3 ,² and morphotropic phase boundary $\text{Pb}(\text{Mg}_{1/3}\text{Nb}_{2/3})\text{O}_3$ - PbTiO_3 .³ The SrTiO_3 (ST) and KTaO_3 (KT) single crystals were purchased in both $\langle 001 \rangle$ and $\langle 011 \rangle$ oriented crystals. The morphotropic phase boundary $\text{Pb}(\text{Mg}_{1/3}\text{Nb}_{2/3})\text{O}_3$ - PbTiO_3 (MPB PMN-PT) single crystals were oriented in the $\langle 001 \rangle$ direction.

The electroceramic compositions of doped ST were synthesized at Xinetics using a procedure adapted from Chen et al. [6]. For each composition, the raw powders purchased at AlfaAesar (Ward Hill, MA) were weighed in stoichiometric ratios and mixed with ethanol. The powder slurry was vibratory milled for 20 hrs and dried. The powder was thermally processed, milled and dried. The resulting powder crystal structure was confirmed by x-ray diffraction and the particle size by laser light scattering. Several difficulties arose trying to process polycrystalline KT and therefore the polycrystalline KT investigations were discontinued.

2.2. Cut and Bond Test Actuators

The test wafers were fabricated using 50 grams of each powder composition mixed with a 2 weight percent PVA binder. After the powder dried, 6.4 and 12.7 mm disks were uniaxially pressed at 140 MPa. Binder burn out and sintering of the disks were performed. The disks were lapped parallel to a desired thickness. The lapped disks were either used in test stacks (6.4 mm) or for capacitance (12.7 mm) measurements.

Capacitance measurements were performed on individual wafers of the synthesized compositions. After lapping, the dimensions of the disks were taken and they were sputter coated with gold. The capacitance of each disk was measured from 20 to 300 K between 0.1–100 kHz at a heating rate of 2°/min. Using the dimensions and capacitance, the dielectric constant as a function of temperature was plotted for each material. The dielectric constant at cryogenic extremes was further related to actuator displacement performance of the same composition.

The lapped wafers were thermally cleaned to remove any organic residue by heating to ~500°C. The wafers were aligned in a fixture with a metal connecting electrode between each wafer pair. The layers were bonded using an adhesive. The tabs on each side were connected using solder to form the negative and the positive bus bars. Electrical leads were connected

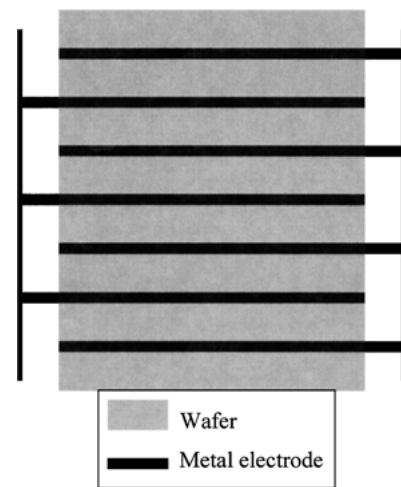


Fig. 3. Illustration of the assembly procedure for a cut and bond stack.

to each of the bus bars followed by conformal coating of the assembled actuator. An illustration of a cut and bond (C&B) actuator is shown in Fig. 3. The cut and bond actuators that passed optical inspection (negligible voids or electrode imperfections) and electrical testing (dc 250 V in He for 5 min at 300 K) were tested at cryogenic extremes.

2.3. Cofired Actuator Development

In the development of a cofiring process, understanding the impact of powder morphology on the tape casting, electrode alignment during the green body forming process, and volumetric shrinkage during densification is crucial to making uniform, homogeneous cofired actuators [7, 8]. The powder production process and potential methods for improving powder properties such as particle size, chemical homogeneity, and batch-to-batch consistency were evaluated to optimize the greenware processing of the powder into electroactive cryogenic ceramics.

The slurry batching and casting process was transitioned from the PMN-based system to the cryogenic powders by careful evaluation of the effect of surface chemistry, particle size and other powder characteristics on the interaction with the tape casting slurry organics. Using the doped SrTiO_3 powder and binders at greater than 40% loadings, slurries that appeared well mixed with no agglomerates were tape cast onto Mylar films. After drying, they were released from the Mylar. The tapes were punched into ~102 mm square

substrates and inspected for surface quality. The tapes that exhibited negligible surface defects were screen-printed.

The screen printing ink used was a thick paste, with shear thinning behavior so that the ink flowed evenly onto the laminate, but held its position once the pattern was formed. The doped SrTiO₃ tapes were screen printed according to a 4 mm diameter by 8 mm length actuator design.

The greenware layers were laminated slightly above the glass transition temperature of the binder system. The lamination schedule was thoroughly evaluated to produce the optimum greenware properties for the cofired cryogenic actuators.

The determination of a binder burnout schedule was complicated by the presence of several lower molecular weight (MW) species such as dispersants and plasticizers (or lower MW components of the resin) that volatilized at temperatures several hundred degrees below the majority of the binder resin. The burnout of the organic in the electrode ink was also considered. Binder burnout profiles were adapted from the knowledge base on PMN processing and were designed to prevent the introduction of defects, such as delaminations, during the removal of the organic.

The sintering cycle was optimized via thermal mechanical analysis (TMA) on the green actuators. The actuator's change in length as a function of temperature and time were measured. Several samples were analyzed using TMA while changing the heating rate. Figure 4 shows the change in length of an actuator as a function of a constant heating rate to the sintering temperature of 1450°C. The onset of shrinkage in the material occurs at a critical temperature at which point the heating rate should be slowed to allow the ceramic to densify uniformly. This avoids introducing temperature and corresponding shrinkage gradients. Due to

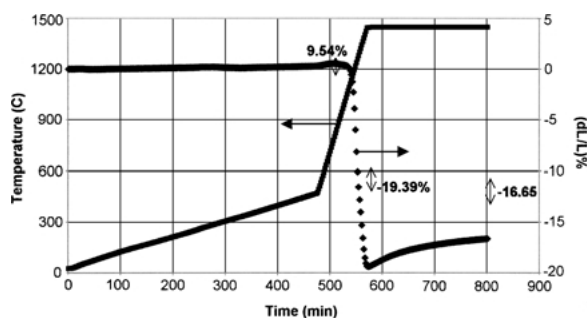


Fig. 4. The TMA analysis of a cofired XiCryo-1 segment.

the TMA results, above 1050°C the sintering rate was decreased by half.

2.4. Cryogenic Actuator Testing Procedures

Tensile strength testing is used to determine the mechanical bond strength between layers in cofired actuators after sintering. Five actuators were chosen from each cofired actuator test batch for tensile testing.

The total thermal expansion was measured for a cofired cryogenic actuator from 10 to 300 K using a modified quartz dilatometer that was placed in a helium cryostat chamber. The C&B actuator stacks that passed the assembly inspection were cryogenically strain tested in the same helium cryostat that was customized to measure capacitance and strain (displacement) as a function of temperature. Due to the constraints of the cryostat, the C&B test actuators were assembled such that the length did not exceed 25.4 mm, with a diameter of 5 mm. The actuators were placed in the cryostat and the temperature was lowered from room temperature to 140 K by the addition of liquid nitrogen then further reduced to 4.2 K by liquid helium. The capacitance (at 1 kHz) and electrical displacement were measured every 5 degrees to 80 K while heating as the coolant evaporated. The field at each temperature ranged from 0 to 1.0 MV/m. The maximum voltage applied was wafer thickness dependent.

As the NASA NAS8-99129 program was initiated, a cryogenic testing facility was designed and built at Xinetics. It contained a large cryogenic chamber to measure optics up to 380 mm in diameter and a small chamber to measure samples up to 32 mm³. The small optical system was used to measure the cofired actuator strain and electrical properties. It was also modified to measure three actuators during one cryogenic cycle. The temperature range for both chambers was 1.4 to 475 K with stability control of ± 0.05 K. A Hewlett Packard 5517C Laser was used to measure the displacement of actuators while a QuadTech 7600 Precision LCR meter was used to measure actuator properties such as capacitance and dielectric loss.

3. Results and Discussion

3.1. Single Crystal C&B Actuator Evaluations

The displacement of each single crystal SrTiO₃ stack peaked at 4.2 K and then dropped dramatically, shown

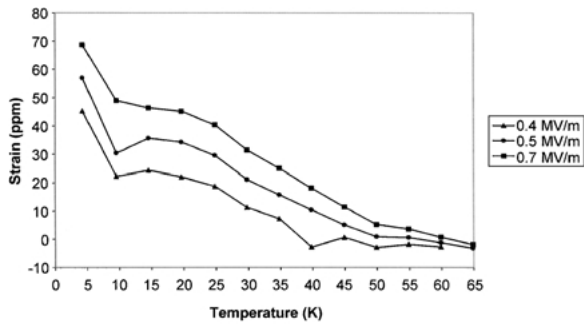


Fig. 5. The cryo-displacement performance of a single crystal SrTiO₃ cut and bond actuator stack.

in Fig. 5. In the 35 to 65 K temperature regime, their strain was too low to be considered as a possible material for a cryogenic deformable mirror. The cryogenic displacement behavior of the KTaO₃ single crystal stacks was very similar to the SrTiO₃ stacks, but they exhibited even lower displacement values. When the cryogenic strain performance was considered for the different crystallographic orientations, the $\langle 001 \rangle$ strain was greater than the $\langle 011 \rangle$ strain. Figure 6 shows a SrTiO₃ cut and bond single crystal wafer actuator stack.

Due to the author's previous experience [9, 10], it was decided to test the performance of a cut and bond actuator stack composed of single crystal MPB PMN-PT wafers poled along the $\langle 001 \rangle$ direction. The cryo-performance of the single crystal PMN-PT stack, shown in Fig. 7, was similar to the room

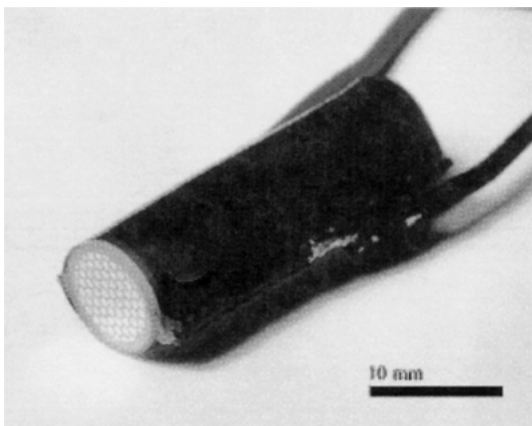


Fig. 6. An assembled 5 mm \times 25.4 mm cut and bond SrTiO₃ actuator fabricated from single crystal wafers.

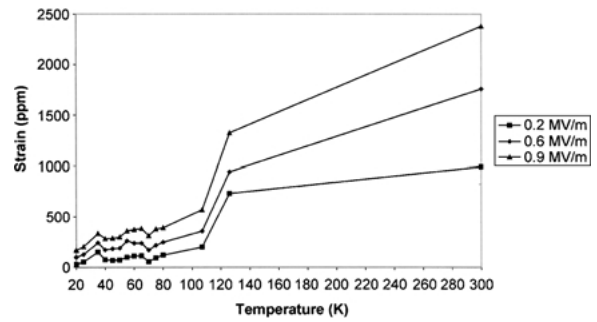


Fig. 7. The cryo-displacement performance of a MPB PMN-PT cut and bond actuator stack.

temperature performance of a room temperature optimized PMN-based actuator stack presently used in our commercial DMs. Therefore, the single crystal MPB PMN-PT would be a possible actuator material for a cryogenic DM. However, a DM composed of single crystal MPB PMN-PT C&B actuator stacks could be cost prohibitive. The growth of the desired single crystal composition, individual crystal orientation, and wafer cutting is time consuming, difficult to handle, and labor intensive. In addition, due to increased wafer thickness, voltages greater than 250 V would be necessary to achieve comparable electric field levels, which is greater than the desired operating voltage in a space environment.

3.2. Cryogenic Strain Measurements of Cut and Bond Electroceramic Actuators

The cryogenic strain performances of twenty four compositions were examined. The performance of the electroceramic C&B stacks varied depending on the concentration (0 to 50 percent) and the general dopant used (compositions are currently proprietary). Figure 8 shows the strain as a function of cryogenic temperature for eight of the C&B actuators tested. One composition exhibited cryogenic strains much greater than the other tested compositions. Several actuators of this doped ST composition were tested and the strain performance was reproducible. It was labeled XiCryo-1, and chosen as the cryogenically active actuator material to be used in the cryogenic deformable mirrors. The XiCryo-1 actuators strain performance was nearly constant across the temperature range of interest (35 to 65 K) and the performance was $\sim 30\%$ of a XiPM-NRE actuator stack at room temperature. The XiCryo-1

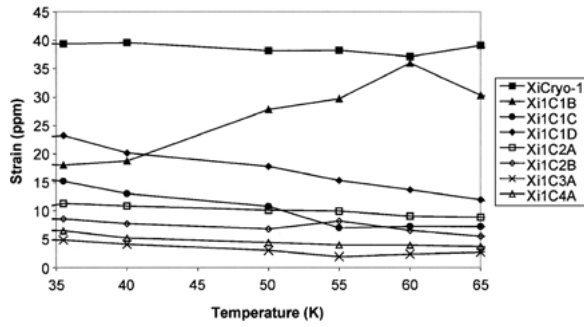


Fig. 8. The cryo-displacement performance of eight cut and bond polycrystalline doped ST actuator stacks.

electroceramic powder composition was employed to fabricate cofired discrete actuators.

Figure 9 shows the displacement performance of the C&B XiCryo-1 actuator stack between 35 and 65 K. The capacitance for XiCryo-1 composition was also measured on several individual wafers at four frequencies from 0.1 to 100 kHz and at a heating rate of 2°/min. The repeatable dielectric constant behavior showed reproducibility of the powder fabrication process. The dielectric constant as a function of temperature for one XiCryo-1 wafer is shown in Fig. 10. It is interesting to note that the XiCryo-1 exhibits a relaxor ferroelectric behavior represented by the shift in T_{max} to higher temperatures and lower values with increasing frequency.

3.3. Cryogenic Strain Measurements of Cofired Electroceramic Actuators

Over twenty blocks of cofired actuator segments were fabricated for various process optimization steps. The cofired segments were characterized using optical inspection and tensile strength. Testing segment tensile

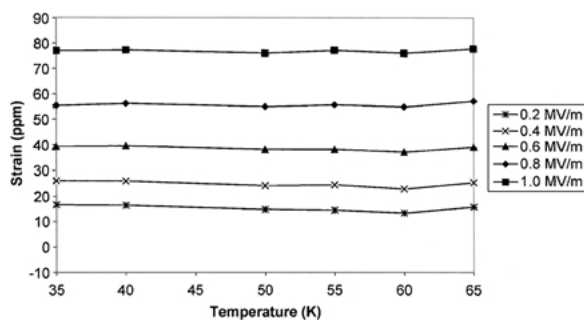


Fig. 9. The cryo-displacement performance of a XiCryo-1 cut and bond actuator stack.

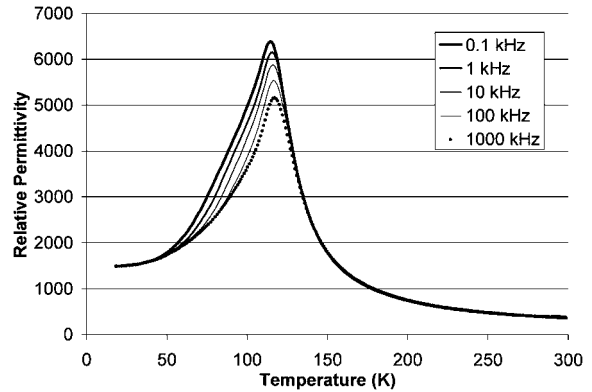


Fig. 10. The dielectric constant as a function of temperature for a XiCryo-1 wafer. Data taken at Alfred University by C. Pagoda and S. Pilgrim (2001).

strength was found to be dependent on the thermal cycles. The optimized thermal cycle produced cofired segments with tensile strengths greater than 27.6 MPa.

Actuator assembly included sizing, striping, wiring, and coating. An actuator electrical test plan was developed for quality control of the cofired actuators. The test were series resistance, parallel resistance, and capacitance at room temperature. Selected cofired actuators were strain tested from 300 to 35 K, then quality control tested again at room temperature. Figure 11 shows a cyclic displacement versus time curve for a cofired XiCryo-1 actuator at 35 K. The actuator exhibited negligible hysteretic behavior similar to PMN at room temperature. Its strain with negative field remained positive, suggesting an electrostrictive material.

The final actuator design was based on the cryogenic 349-channel discrete actuator DM requirements. The 4 mm diameter was due to the 7 mm interactuator spacing requirement for the DM. Three XiCryo-1 segments were bonded together to achieve the 3.0 μm

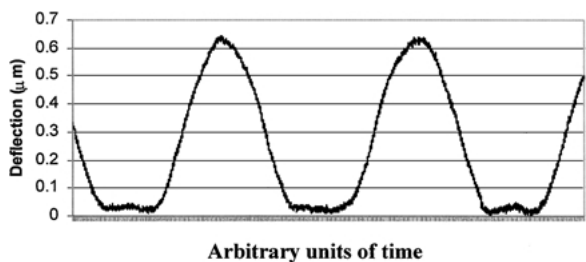


Fig. 11. The XiCryo-1 exhibited positive strain with negative field, thus electrostrictive behavior. It was cycled at 5.0 Hz from 75 to -25 V at 75 K. The X-axis is arbitrary time.

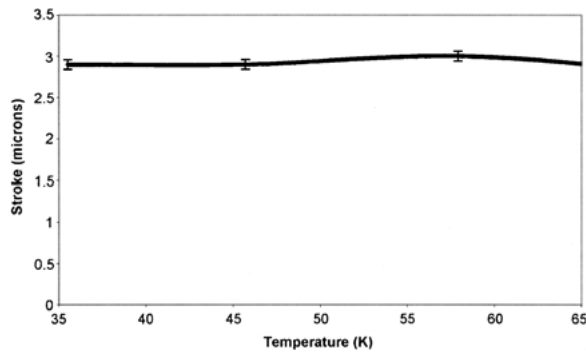


Fig. 12. The cryo-displacement performance of a XiCryo-1 cofired actuator stack. It exhibited $3\ \mu\text{m}$ of displacement at 150 V. Error bars represent 2 percent deviation.

displacement goal at 150 V. Displacement performance of cryogenic cofired actuators was nearly constant from 35 to 65 K as shown in Fig. 12. The 349 XiCryo-1 actuators plus spares for the DM are shown in Fig. 13. The operating voltage can be further reduced in future designs by decreasing the ceramic layer thickness.

3.4. Cryogenic Cofired Actuator Quality Control

Since actuators in a DM must push and pull on the mirror surface, tensile strength testing of the cofired actu-

ator segments is a critical actuator quality control measurement. Since it was unknown if tensile strength at 300 K was comparable at 35 K, a sample fixture was designed to test the tensile strength of the cryogenic actuators at 35 K. A single segment of XiCryo-1 actuator was bonded to a silicon tab with cryogenic epoxy. Due to the cost of cryogenic testing, only two samples were tensile strength tested at 35 K. Both exhibited values greater than 27.6 MPa. The cryogenic tensile tests showed that tensile strength of the XiCryo-1 actuators at 35 K are quite similar to 300 K tensile strength measurements.

The total thermal expansion was measured for cofired and cut and bond XiCryo-1 actuators from 300 to 35 K. For the C&B actuators it was approximately $-2500\ \text{ppm}$ and for the cofired stack approximately $-1500\ \text{ppm}$. The variation in values was attributed to the large number of epoxy joints in the C&B actuators. The coefficient of thermal expansion for the actuators was a significant materials property in the cryogenic DM design decisions.

4. Summary

Over twenty years of development was necessary to achieve today's commercialized PMN cofired actuators that are used in Xinetics' room temperature deformable

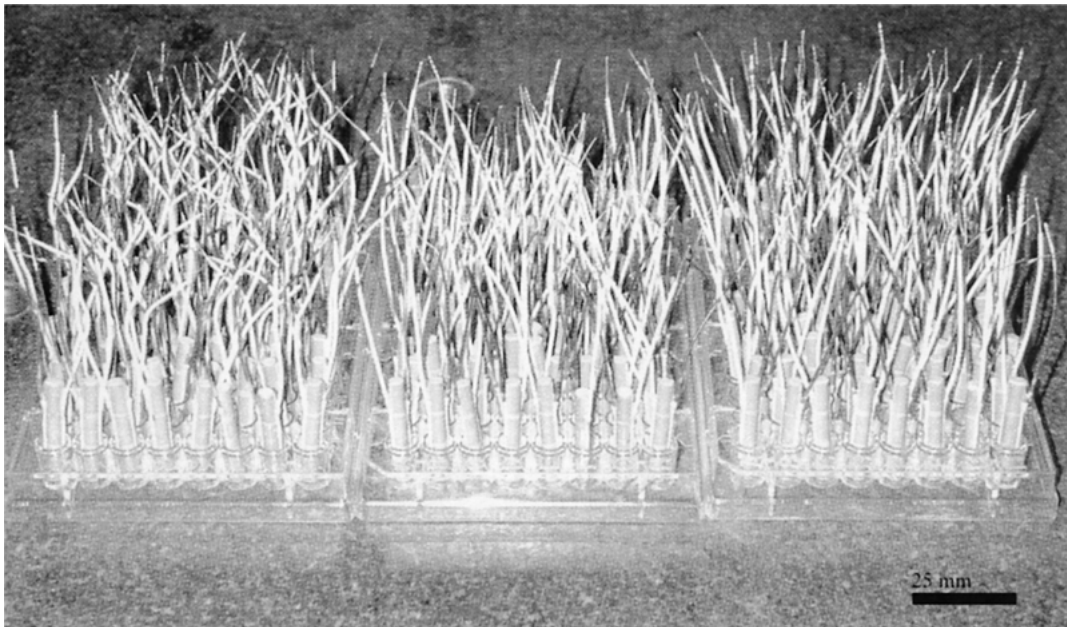


Fig. 13. A display of the 349 actuators that were assembled in the 349-ch discrete actuator DM. The actuators are 4 mm in diameter by 24 mm in length.

mirrors. The developments occurred in a sequence of stages such as powder synthesis and property characterization, cut and bond (C&B) assembly optimizations and cofired process development and implementation. A similar sequence of stages was followed in the development of cofired cryogenic actuators, but in only two years. The cryogenic strain of over twenty four compositions were measured that were composed of single crystal KTaO_3 , SrTiO_3 , MPB PMN-PT, and polycrystalline doped SrTiO_3 . One composition, XiCryo-1, was down selected as the electrostrictive cryogenic electroceramic to operate between 35 and 65 K. The XiCryo-1 composition was fabricated into over 349 discrete cofired actuators that were assembled into a cryogenic deformable mirror pathfinder that was designed to meet the needs of the Next Generation Space Telescope. The actuators exhibited negligible hysteretic response suggesting an electrostrictive material between 35 and 65 K and displacement of $3 \mu\text{m}$ at 150 V, meeting the actuator design requirements.

Acknowledgments

The authors are grateful for the funding of this development program by NASA Marshall Space Flight Center under Phase II and III NASA SBIR contract numbers NAS8-98073 and NAS8-99129, respectively. We would also like to thank the Xinetics team that worked on these programs. They did a great job in the realization of a cryogenic deformable mirror technology specific to the needs of NGST.

Since this is a special issue of the Journal of Electroceramics in honor of the career of Professor Robert E.

Newnham, Drs. Mulvihill and Bagwell want to especially thank him for his mentoring, teaching, advising and friendship.

Notes

1. Atomergic Chemetal Co., Farmingdale, NY.
2. Commercial Crystal Lab, Inc., Naples, FL.
3. H.C. Materials, Urbana, IL.

References

1. H.S. Stockman, *The Next Generation Space Telescope: Visiting a Time When Galaxies were Young* (The Association of Universities for Research in Astronomy Inc., Washington D.C., 1997), p. vii.
2. J. Fanson and M. Ealey, *Proceedings SPIE*, **1920**, 306 (1993).
3. R.K. Tyson, *Introduction to Adaptive Optics* (SPIE-The International Society for Optical Engineers, Washington, 2000), p. 54.
4. K. Uchino, *Ferroelectric Devices* (Marcel Dekker, Inc. New York 2000), p. 74.
5. K.H. Hellwege and A.M. Hellwege (Eds.), *Landolt-Börnstein: Numerical Data and Functional Relationships in Science and Technology: Group III for Ferroelectrics and Related Substances* (Springer-Verlag, Berlin Heidelberg New York, 1981), Vol. 16, p. 283.
6. J.S. Chen, R.J. Young, and T.B. Wu, *Commun. Amer. Ceram. Soc.*, **70**(10), C-260 (1987).
7. R.E. Mistler and E.R. Twiname, *Tapcasting* (The American Ceramic Society, Westerville, OH, 2000), p. 209.
8. L. Sheppard (Ed.), *Amer. Ceram. Soc. Bull.*, **72**(3), 451 (1993).
9. M.L. Mulvihill, S.E. Park, G. Risch, Z. Li, K. Uchino, and T.R. Shrout, *Jpn. J. Appl. Phys.*, **35**, 3984 (1996).
10. M.L. Mulvihill, L.E. Cross, and K. Uchino, *Proceedings for Eighth European Meeting on Ferroelectrics, Ferroelectrics*, **186**, 325 (1996).